NASA TECHNICAL NOTE

NASA TN D-7057

NASA TN D-7057

PROPERTIES OF CRYSTALLINE BISMUTH SELENIDE AND ITS USE AS A HALL EFFECT MAGNETOMETER

by John A. Woollam, Harry Beale, and Ian L. Spain

Lewis Research Center

Cleveland, Ohio 44135

NATIONAL AERONAUTICS AND SPACE ADMINISTRATION • WASHINGTON, D. C. • NOVEMBER 1972

1. Report No. NASA TN D-7057	2. Government Accession No.	3. Recipient's Catalog No.
4. Title and Subtitle PROPERTIES OF CRYSTALLINE BISMUTH SELENIDE AND ITS USE AS A HALL EFFECT MAGNETOMETER		5. Report Date November 1972 6. Performing Organization Code
7. Author(s) John A. Woollam, Lewis Research Center; Harry Beale and Ian L. Spain, University of Maryland		8. Performing Organization Report No. E-6805
9. Performing Organization Name and Address Lewis Research Center National Aeronautics and Space Administration Cleveland, Ohio 44135		10. Work Unit No. 503-10 11. Contract or Grant No.
12. Sponsoring Agency Name and Address National Aeronautics and Space Administration Washington, D.C. 20546		13. Type of Report and Period Covered Technical Note 14. Sponsoring Agency Code

15. Supplementary Notes

16. Abstract

Single crystals of n-type Bi_2Se_3 grown by the Bridgman technique are found to make excellent Hall effect magnetometers. Plots of Hall resistivity ρ_{yx} against magnetic field B to 10 tesla are linear to within 1 percent. Furthermore, the slope of the ρ_{yx} against B curve varies by about 1 percent in the region 1.1 to 35 K and by less than 20 percent in the region 1.1 to 300 K. Analysis of galvanomagnetic measurements indicate the samples have semimetallic densities of $\sim 10^{25}/m^3$, with (at least) two-band conduction and have near carrier compensation. Reflectivity measurements suggest a band gap of approximately 0.08 eV for our samples. The temperature dependence of mobility is also measured. A series of 50 direct immersions into liquid helium and liquid nitrogen demonstrate the reliability of Bi_2Se_3 magnetometers for cryogenic use.

17. Key Words (Suggested by Author(s))	18. Distribution Statement
Bismuth selenide; Hall effect; Galvanomagnetic effects; Semiconductor; Mobility; Carrier concentrations; Two-band conduction; Magnetometer	Unclassified - unlimited

19. Security Classif. (of this report)	20. Security Classif. (of this page)	21. No. of Pages	22. Price*
Unclassified	Unclassified	21	$3.00

* For sale by the National Technical Information Service, Springfield, Virginia 22151

PROPERTIES OF CRYSTALLINE BISMUTH SELENIDE AND ITS USE AS A HALL EFFECT MAGNETOMETER

by John A. Woollam, Harry Beale*, and Ian L. Spain†

Lewis Research Center

SUMMARY

Single crystals of both n- and p-type Bi_2Se_3 grown by the Bridgman technique are found to make excellent Hall effect magnetometers. Plots of Hall resistivity ρ_{yx} against magnetic field B to 10 tesla deviate from linearity by less than 1 percent and show no Shunbnikov-de Haas oscillations below 10 tesla at any temperature. The slope of the ρ_{yx} against B curve varies by about 1 percent in the region 1.1 to 35 K and by less than 20 percent in the region 1.1 to 300 K. Quenching tests demonstrate magnetometer reliability for cryogenic applications.

From galvanomagnetic data the mobility and the carrier density as a function of temperature are found. Optical reflectivity experiments suggest a band gap of ~0.08 eV. Analysis of all data indicates that the samples are nearly compensated (requiring at least two-band conduction) and have semimetallic carrier density of $\sim 10^{25}$ per cubic meter. Mobilities on the order of 10^{-2} square meter per volt per second at 300 K increase by greater than a factor of three at 1.1 K.

INTRODUCTION

NASA currently has operating and under construction several superconducting magnets (ref. 1) to be used for plasma physics studies and other research related to space power and propulsion applications. Accurate and convenient measurement of high magnetic fields becomes more difficult as higher field magnets and superconducting solenoids are developed. Nuclear magnetic resonance is very accurate, but high homogeneity of the magnetic field is needed (ref. 2), and it is often difficult to include a nuclear resonance measurement at the same time that other measurements are performed (ref. 3).

*Research Associate, University of California, Los Angeles, California.

†Associate Professor of Chemical Engineering, University of Maryland, College Park, Maryland.

Copper magnetoresistors have nearly linear output with field at high fields, but their calibration is very temperature sensitive and a quadratic component is present in the output at low field (ref. 4). Hall effect devices are small (dimensions on the order of a few mm) and quite linear in field at high temperature. The best Hall devices available up to now are films of indium arsenide (ref. 5), but these are frequently unreliable upon cycling to low temperature and often exhibit Shubnikov-de Haas oscillations at low temperatures (ref. 6).

We have found single crystals of Bi_2Se_3 grown by the Bridgman technique to be ideal magnetometers in magnetic fields to at least 10 tesla and over a wide range of temperature. In this report, the measured Hall resistivity is reported for a representative p-type sample as a function of temperature from 1.2 to 300 K and as a function of magnetic field to 10 tesla. Magnetoresistivity was also measured and is used with the Hall effect results to help characterize the magnetometer material. A series of direct immersions from 300 K into cryogenic liquids demonstrated reliability for low temperature uses.

In addition to its use as a magnetometer, which we have demonstrated in this report, Bi_2Se_3 is of practical interest for several other reasons. The thermoelectric figure of merit is high (ref. 7) for both Bi_2Se_3 and Bi_2Te_3 making these materials useful for thermoelectric energy conversion. Secondly, the band gap is found near 0.08 eV in our samples. Thus, this material is of possible interest for infrared radiation detectors (ref. 8). The optimization of the material for these applications will require further study and improvement of the electronic properties. This report describes studies of electronic and optical properties of n- and p-type single crystals in high magnetic fields and over a wide range of temperatures. Hashimoto (ref. 9), and Caywood and Miller (ref. 10) have studied galvanomagnetic properties, but their studies were limited to temperatures above 80 K and to low magnetic fields. Optical studies were made by Greenaway and Harbeke (ref. 11) who find an energy band gap of $\cong$0.16 eV in their samples.

MATERIALS PREPARATION AND MEASUREMENT TECHNIQUE

The starting materials for this series of experiments were 99.999 percent pure bismuth and selenium shot. To make p-type samples, 100 grams of material were weighed out, to an accuracy of $\pm$0.0005 gram, for a composition of 60.25 atomic percent selenium and 39.75 atomic percent bismuth. The mixture of shot was placed in a vycor ampoule, evacuated to approximately 10^{-5} millimeters of mercury and sealed. The ampoule was maintained at 850° C (the melting temperature is 710° C) for 12 hours in a furnace vibrating at approximately 8 hertz. Samples were made using a Bridgman furnace (ref. 12), with a growth rate of 0.012 meter per hour. The product was a polycrystalline boule, 0.07 meter long by 0.015 meter diameter. Grains were large in cross section and typically the length of the boule. By chemical analysis, the composition varied from 39.97

atomic percent bismuth near the bottom of the boule to 39.82 atomic percent near the top. The boule was sectioned into 0.018 meter lengths using a wire saw with a diamond impregnated wire. One of these shorter cylinders from the upper end of the boule was etched, using a mixture of methanol and bromine, to reveal the grain boundaries and then cleaved to produce single crystals. The predominant cleavage plane was the plane perpendicular to the trigonal axis.

Specimens were cut by sand erosion to the shape of a conventional Hall resistivity sample as shown in figure 1. Typical sample dimensions were 0.05 by 0.14 by 0.80×10^{-2} meter. Bi_2Se_3 has a trigonal unit cell and exhibits the $R\bar{3}m$ symmetry. If the z-axis is taken as the trigonal axis and the x-axis as the long axis of the sample, then the specimens were oriented and cut so the xz-plane was one of the three equivalent reflection planes. The samples were again etched and re-examined for cracks between the layer planes using a simple light microscope. Leads were attached with a conductive epoxy, carefully covering the entire tip region. This procedure eliminated any spurious effects due to the pronounced layer structure of the crystal. The previously described procedure produced p-type material as grown; n-type was produced in a second boule nominally 0.05 percent bismuth rich by annealing for 48 hours at 600° C.

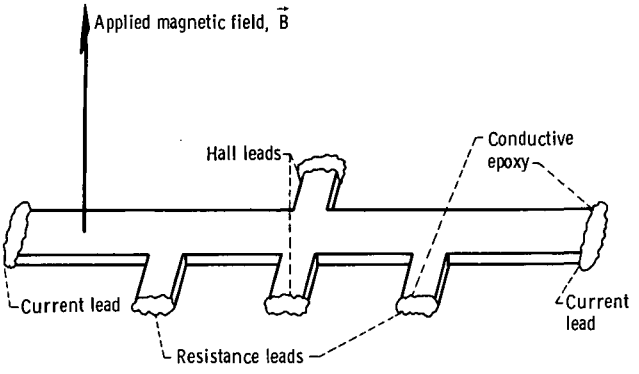

Figure 1. - Sample geometry showing tabs for attachment of electrical leads with conductive epoxy. (Electroplated copper was also successful.)

A dc constant current supply, having an output calibrated to one part in 10^5, provided currents of typically 100 milliamperes. Voltages were measured by using a dc amplifier with gains accurate to one part in 10^5 and were plotted on a calibrated x-y recorder. A water-cooled solenoid, calibrated against a rotating coil magnetometer and a standard magnet, provided the magnetic field. Field values ranged between zero and ±10 tesla (1 tesla = 10 kG), with the field oriented along the trigonal axis of the sample. Temperatures between 1.1 and 300 K were achieved by using liquid helium and liquid nitrogen with a heater-controlled system employing a gallium arsenide temperature sensor (ref. 13).

THEORETICAL CONSIDERATIONS

The experimentally measured quantities were the Hall resistivity ρ_{xy} and the magnetoresistivity ρ_{xx}. For the magnetic field along the trigonal axis of the $R\bar{3}m$ structure of Bi_2Se_3, the conductivity tensor elements σ_{xx} and σ_{xy} can be obtained from the following relations:

$$\sigma_{xx} = \frac{\rho_{xx}}{\rho_{xy}^2 + \rho_{xx}^2} \tag{1}$$

and

$$\sigma_{xy} = \frac{-\rho_{xy}}{\rho_{xy}^2 + \rho_{xx}^2} \tag{2}$$

(Symbols are defined in appendix A.) These conductivity tensor elements can be expanded (ref. 14) as

$$\sigma_{xy} = \sum_{i=1}^{r} \frac{n_i e_i \left(\frac{B}{B_i^2}\right)}{1 + \left(\frac{B}{B_i}\right)^2} \alpha_i \tag{3}$$

and

$$\sigma_{xx} = \sum_{i=1}^{r} \frac{\frac{n_i |e_i|}{B_i}}{1 + \left(\frac{B}{B_i}\right)^2} \beta_i \tag{4}$$

where the sum is over the different carriers and where n_i is the concentration of the i^{th} carrier, e_i is the charge of the i^{th} carrier, B is the magnetic flux density, and α_i and β_i are degeneracy parameters, the values of which do not usually deviate from

unity by greater than 20 percent. For the remaining development of this section, these parameters will be taken as unity, as a simplification. By definition,

$$B_i = \frac{1}{\mu_i} \tag{5}$$

where μ_i is the mobility of the i^{th} carrier.

The simplest analysis allows the use of a one carrier model. In this case, only two quantities are necessary to specify the system, the carrier concentration and charge mobility. If

$$\frac{\Delta\rho}{\rho_o} \equiv \frac{\rho_{xx}(B) - \rho_{xx}(B = 0)}{\rho_{xx}(B = 0)} \tag{6}$$

then the magnetoconductivity mobility is

$$\mu_c = \left(\frac{\Delta\rho}{\rho_o B^2}\right)^{1/2} \quad m^2/(V)(sec) \tag{7}$$

where B is in tesla and V is in mks practical volts. Equation (7) follows from equation (4) for a one-band system assuming $\rho_{xx} >> \rho_{xy}$. The latter was experimentally found to be true in Bi_2Se_3. However, as will be shown, Bi_2Se_3 can be described as a two-band system. The carrier concentration is

$$n = \frac{\sigma_{xx}(B = 0)}{|e|\mu_c} \tag{8}$$

which follows from equation (4) if $B << B_i$, which was also found experimentally in Bi_2Se_3. The system is then determined. However, another independent operational relation is available from the Hall parameter. With

$$R_H(B) = \frac{\rho_{xy}}{B} \tag{9}$$

the Hall mobility is

$$\mu_H = R_H \sigma_{xx}(B = 0) \tag{10}$$

Therefore three relations (eqs. (7), (8), and (10)) exist for the determination of two quantities (n and μ). These relations can be used to assess the applicability of the chosen model (either single carrier or multicarrier). If the quantities μ_c and μ_H differ by less than say 20 percent, then it may be inferred that the single carrier model is applicable to the experimental data. Such a small discrepancy implies the degeneracy parameters α and β deviate from unity. A small discrepancy is also expected dependent on the predominant scattering mechanism. However, if the disparity between the μ_c and μ_H is larger, then it may be inferred that more than one carrier is responsible for the measured galvanomagnetic properties. This results from equations (7) and (10) being valid for the one carrier case only.

Consider a two carrier model. If the degeneracy parameters are again taken as unity, then only four quantities are necessary to specify the system, instead of eight. With the definitions

$$a = \frac{n_2}{n_1} \tag{11}$$

and

$$b = \frac{\mu_1}{\mu_2} = \frac{B_2}{B_1} \tag{12}$$

the two carrier analogs of equations (7), (8), and (9) are, from Soule (ref. 15),

$$\mu_c = \left(\frac{a+b}{1+b}\right)\left(\frac{1}{ab}\right)^{1/2}\left(\frac{\Delta\rho}{\rho_o B^2}\right)^{1/2} \times 10^4 \quad m^2/(V)(sec) \tag{13}$$

$$\sigma_{xx}(B = 0) = n_1|e|\mu_1\left(1 + \frac{a}{b}\right) \tag{14}$$

and

$$R_H(0) = \frac{1}{n_1 e}\frac{(a-b)^2}{(a+b)^2} \tag{15}$$

for $B \ll B_i$. For equation (15), $e_2 = -e_1$. Therefore, only three relations exist (eqs. (13), (14), and (15)) for the determination of four quantities (μ_1, μ_2, n_1, and n_2). An

additional relation can be obtained from the high field dependence of the Hall parameter. This may be accomplished by fitting to the magnetic field dependence of $R_H(B)$ if data is only available in the range $B \lesssim B_i$; or if data to the high field limit ($B >> B_i$) is available, then with the aid of the formula

$$R(\infty) = \frac{1}{|e|(n_2 - n_1)} \tag{16}$$

Equations (13) to (16) can then be used to determine the four unknowns.

RESULTS

The data discussed in this report are on p-type material. We also have studied n-type materials, and the results are very similar. All of the discussion concerning magnetometer applications is equally valid for both n- and p-type.

Representative plots of the Hall resistivity as a function of magnetic field B for various temperatures are shown in figure 2 for the p-type material. Over the range of field from zero to 8.0 tesla, the variation of ρ_{yx} is linear in B. Figure 3 displays the variation in p-type material of ρ_{yx} with temperature at a fixed field of 7.0 tesla. This is essentially a plot of the temperature dependence of the magnetometer sensitivity. In table I are listed the values of the Hall and magnetoconductivity mobilities which were computed using equations (7) and (10). Clearly these quantities differ significantly, indicating the presence of more than one carrier.

Figure 4 is a composite, displaying the temperature dependence for p-type material of $\rho_{xx}(o)$ and also the magnetic field dependence of $\rho_{xx}(B)$ for various temperatures. The weak field dependence of ρ_{xx} is very evident, being ~15 percent at 4.2 K and ~2 percent at 300 K at 7 tesla. It is also evident that there is a quadratic component of field dependence. From figures 3 and 4, note that ρ_{xy} is always less than 0.8 percent of ρ_{xx}. The resistivity ratio $\rho_{xx}(300\ K)/\rho_{xx}(4.2\ K) = 4$ for this sample. Equation (6) was used to compute the magnetoresistance which is shown in figure 5. The magnetoconductivity mobility was computed using equation (7) and is also shown in figure 5. An average carrier concentration was computed using equation (8) and is shown in figure 6.

Finally, we have measured the reflectivity as a function of wavelength at 300 K. A small rise in reflectivity near 15 micrometers suggests the presence of a band gap of 0.08 eV, which is considerably smaller than the value of 0.16 eV found by Greanaway and Harbeke (ref. 11).

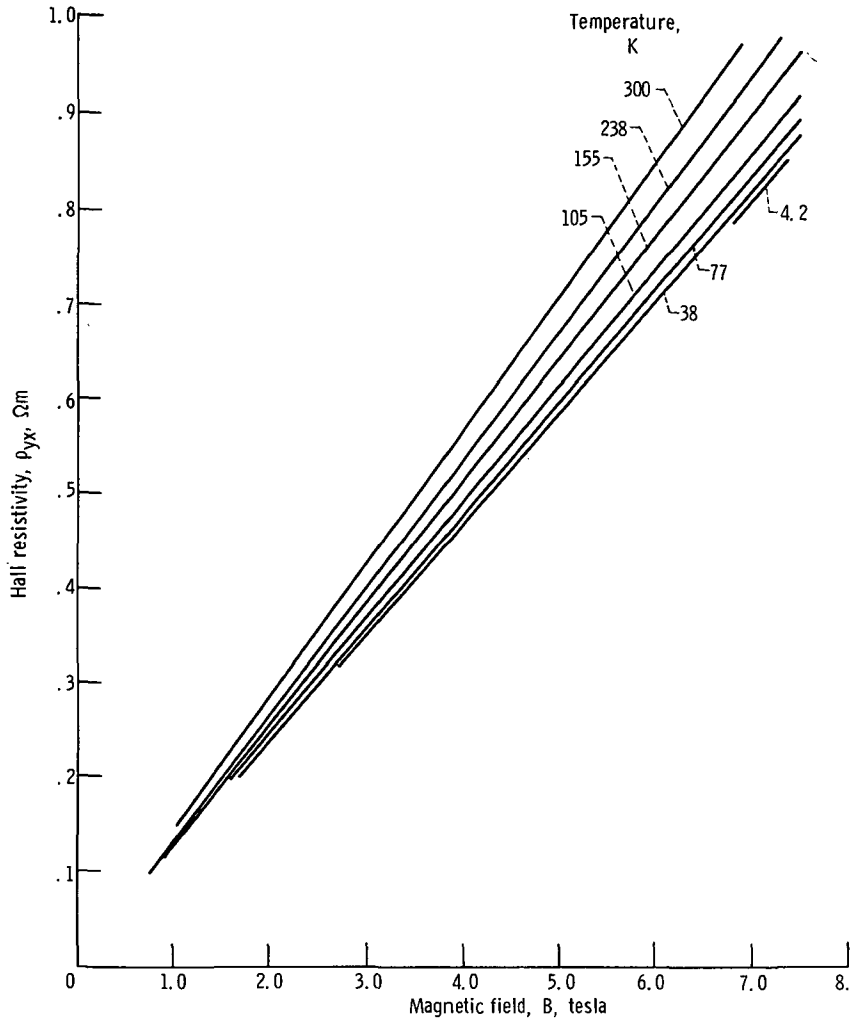

Figure 2. - Hall resistivity of p-type sample at various temperatures.

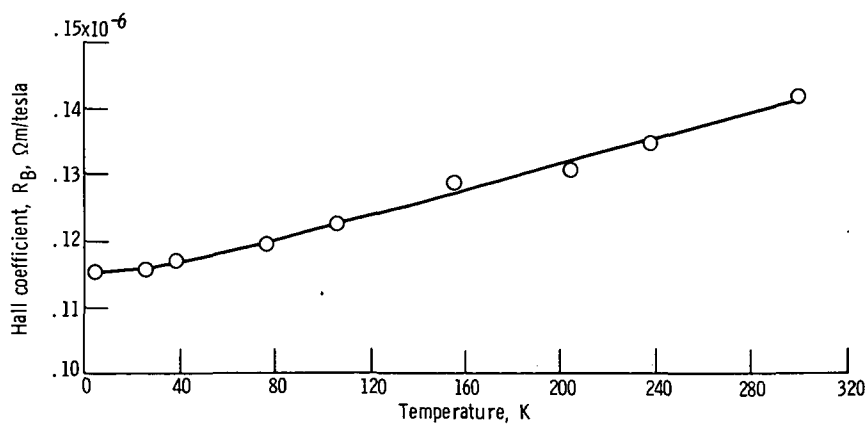

Figure 3. - Hall constant as a function of temperature at a fixed field.

TABLE I. - HALL MOBILITIES, CONDUCTIVITY MOBILITIES, CONDUCTIVITIES, AND TOTAL CARRIER DENSITY FOR A REPRESENTATIVE p-TYPE SAMPLE FROM AN UNANNEALED BOULE

Temperature, K	Hall mobility, μ_H, $m^2/(V)(sec)$	Magnetoconductivity mobility, μ_c, $m^2/(V)(sec)$	Conductivity at zero field, $\sigma_{xx}(0)$, $(\Omega m)^{-1}$	Net carrier density, $n_1 + n_2$, m^{-3}
4.2	1.3×10^{-2}	4.75×10^{-2}	1.11×10^{5}	1.5×10^{25}
38	1.3	4.40	1.11	1.6
78	.88	3.50	.714	1.3
105	.79	3.10	.589	1.2
155	.60	2.40	.455	1.2
198	---	2.3	.385	1.1
238	---	2.1	.345	1.03
300	.42	1.75	.286	1.00

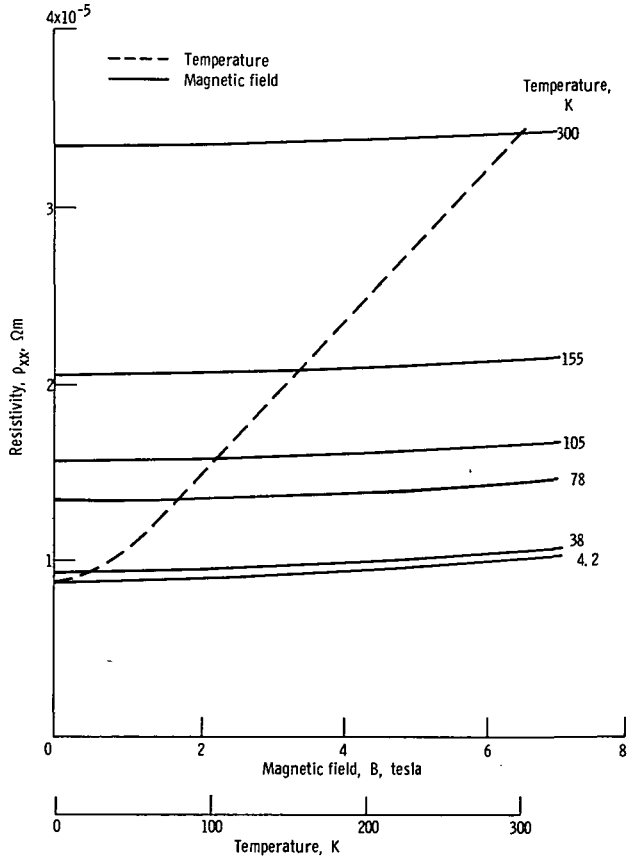

Figure 4. - Resistivity plotted against magnetic field for various temperatures and against temperature.

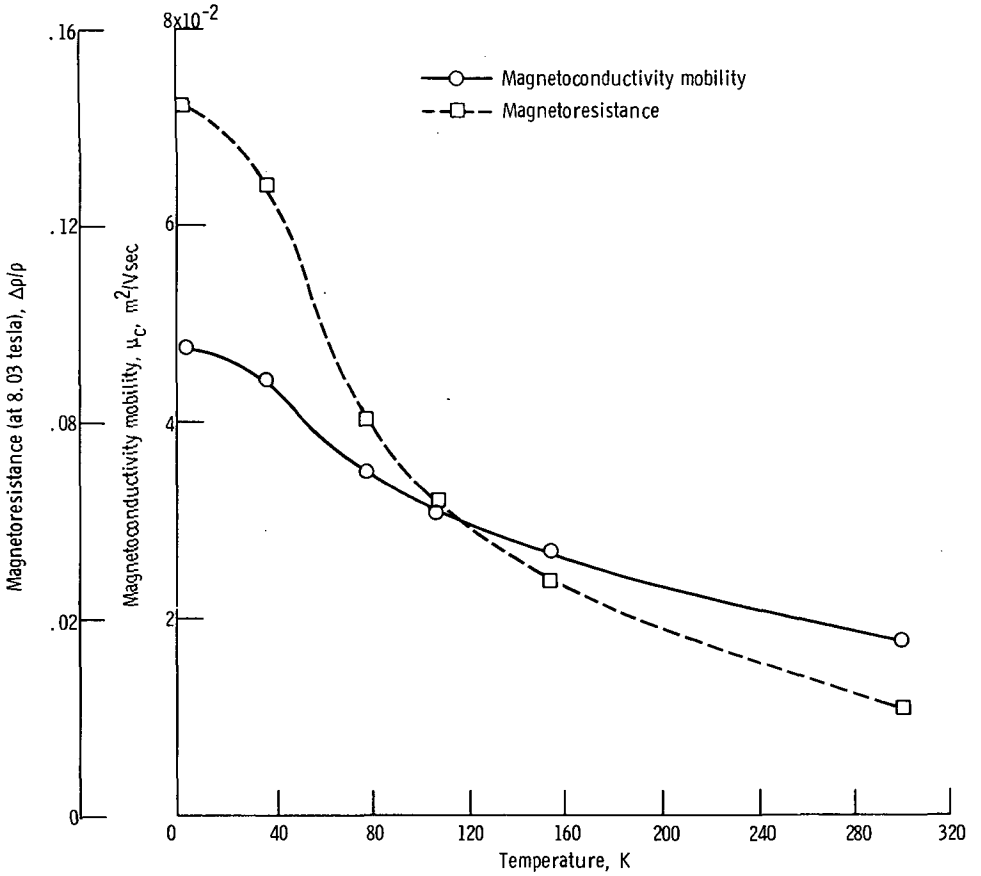

Figure 5. - Mobility and magnetoresistance plotted against temperatures.

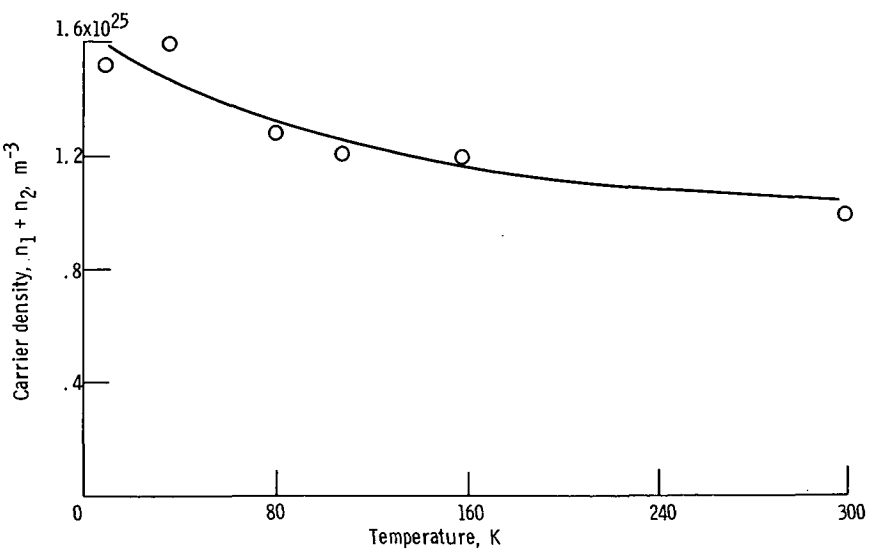

Figure 6. - Carrier concentration $n_1 + n_2$ plotted against temperature for p-type Bi_2Se_3.

DISCUSSION OF RESULTS

Applications as a Magnetometer

The most significant results of the present investigation for practical applications, is that the Hall resistivity ρ_{yx} is linear in B, within 1 percent, over the temperature range 1.1 to 300 K. The data for several temperatures are conveniently displayed in figure 3.

The linear Hall resistivity with magnetic field may be explained using the theory discussed earlier, as will now be shown. The result of inverting equations (1) and (2) is

$$\rho_{yx} = \frac{\sigma_{xy}}{\sigma_{xx}^2 + \sigma_{xy}^2} \tag{17}$$

and

$$\rho_{xx} = \frac{\sigma_{xx}}{\sigma_{xx}^2 + \sigma_{xy}^2} \tag{18}$$

These equations may be expanded by using equations (3) and (4) as (see appendix B for details):

$$\rho_{yx} = \frac{\frac{B}{b^2}(b^2 - a) + B\left(\frac{B}{bB_1}\right)^2 (1 - a)}{n_1 e\left\{\left[\frac{M_2}{M_1} + \frac{2a}{b} + \left(\frac{a}{b}\right)^2 \frac{M_1}{M_2}\right] + \left(\frac{B}{B_1}\right)^2 \left[\frac{M_2}{M_1} - \frac{2a}{b^2} + \left(\frac{a}{b^2}\right)^2 \frac{M_1}{M_2}\right]\right\}} \tag{19}$$

and

$$\rho_{xx} = \frac{B_1 \frac{1}{b}(a + b) + \left(\frac{B}{bB_1}\right)^2 (ab + 1)B_1}{n_1 e\left\{\left[\frac{M_2}{M_1} + \frac{2a}{b} + \left(\frac{a}{b}\right)^2 \frac{M_1}{M_2}\right] + \left(\frac{B}{B_1}\right)^2 \left[\frac{M_2}{M_1} - \frac{2a}{b^2} + \left(\frac{a}{b^2}\right)^2 \frac{M_1}{M_2}\right]\right\}} \tag{20}$$

where

$$M_i = 1 + \left(\frac{B}{B_i}\right)^2 \tag{21}$$

Consequently, whether ρ_{xy} has strong linear or cubic field dependence is controlled by the quantities (1 - a) and (b^2 - a). As "a" approaches unity (meaning the material is almost completely compensated, $n_1 \approx n_2$), ρ_{xy} will become nearly linear in field. The parabolic behavior of ρ_{xx} is demonstrated by equation (20). Again, linearity of ρ_{xy} with B and a quadratic component of ρ_{xx} with B were observed experimentally. The following experimental results will be used to evaluate B_1, B_2, and a in equations (19) and (20):

$$\left.\frac{R_H(B) - R_H(0)}{R_H(0)}\right|_{\substack{B=7 \text{ tesla} \\ T=4.2 \text{ K}}} \simeq 0.015 \tag{22}$$

$$\left.\frac{\rho_{xx}(B) - \rho_{xx}(0)}{\rho_{xx}(0)}\right|_{\substack{B=7 \text{ tesla} \\ T=4.2 \text{ K}}} \simeq 0.15 \tag{23}$$

$$\frac{\rho_{xx}(B)}{\rho_{xy}(B)} \geq 0.008 \tag{24}$$

From the measured values of mobility (table I) the B_i's are large compared with the largest B used (see eq. (5)). Thus equations (19) and (20) yield

$$\frac{R_H(B) - R_H(0)}{R_H(0)} \simeq \frac{B^2}{B_1^2} \frac{(1 - a)}{(b^2 - a)} \tag{25}$$

$$\frac{\rho_{xx}(B) - \rho_{xx}(0)}{\rho_{xx}(0)} \simeq \frac{1}{b}\left(\frac{B}{B_1}\right)^2 \frac{(ab + 1)}{(a + b)} \tag{26}$$

$$\frac{\rho_{xx}(B)}{\rho_{xy}(B)} \simeq \frac{\left[b(a + b) + \left(\frac{B}{B_1}\right)^2 (ab + 1)\right] B_1}{B(b^2 - a)} \tag{27}$$

There are then three equations in three unknowns, a, B_1, and B_2 which could be solved. To simplify solution, various trial values of a and b were chosen and varied until equations (25), (26), and (27) fit results (22), (23), and (24) to within a few percent. Incompatibility of solutions for $a \ll 1$ was found. But with $a \cong 1$, the following results were found for a temperature of 4.2 K:

$$\left.\begin{aligned} a &\simeq 0.99974 \\ B_1 &\simeq 18.00 \text{ tesla} \\ B_2 &\simeq 18.02 \text{ tesla} \\ b &\simeq 1.001184 \end{aligned}\right\} \tag{28}$$

Thus the linearity of ρ_{xy} with B (see eq. (19)) results principally from the near compensation of carriers ($n_1 \cong n_2$ or $a \cong 1$). By using equations (28) and (5), the mobilities should then be

$$\mu_1 \simeq \mu_2 \simeq 0.056 \text{ m}^2/(\text{V})(\text{sec}) \tag{29}$$

Experimental values of μ for various temperatures are listed in table I.

Nearly as significant as the linearity of ρ_{yx} with B and the absence of the Shubnikov-de Haas effect below 10 tesla in Bi_2Se_3 is the very small temperature variation of the slope of ρ_{yx} against B. This means that a magnetometer needs only to be calibrated at a few temperatures (e.g., 4.2, 78, and 300 K) and can be used for accurate field measurements over wide ranges of temperature. This property contrasts with the strong temperature dependence of some presently used Hall effect magnetometers (ref. 5), and all copper magnetoresistance magnetometers (ref. 4). Copper magnetoresistance typically changes by 100 percent over the range of 35 to 4.2 K.

A Hall effect magnetometer has an inherent advantage over magnetoresistance magnetometers in that the magnetoresistance of most materials is proportional to B^2 at low B. This is true, for example, in copper magnetometers which are fairly linear only above a magnetic field of typically 0.2 to 1.0 tesla (ref. 4).

The most serious problem with previous Hall magnetometers was the change in characteristics, or complete failure, after cycling to cryogenic temperatures. For this reason Bi_2Se_3 probes have been cycled in the following manner:

(1) Ten direct immersions into liquid nitrogen from 300 K with the Hall resistivity measured to ±5 tesla each time the probe was in liquid. All values of ρ_{yx} at 5 tesla were within 1 percent of each other.

(2) Ten direct immersions into liquid helium from 300 K with the Hall resistivity

measured to ±5 tesla each time the probe was in liquid. All values of ρ_{yx} at 5 testla were within 0.2 percent of each other.

(3) Thirty direct immersions into liquid nitrogen from 300 K with ρ_{yx} measured in liquid helium at 5 tesla after each 10 immersions into liquid nitrogen. All values of ρ_{yx} at 5 testla were within 0.3 percent of each other.

Characterization of the Material

In the last section it was demonstrated that the data can be interpreted by a two-band model where $a \cong 0.999$, $B_1 \cong B_2 \cong 18$ tesla, and mobilities are ~0.056 square meter per volt per second. Figure 4 shows that the total resistivity decreases by a factor of four on going from 300 to 1.2 K, and figure 5 shows that mobility increases by a factor of about three as temperature decreases. Elementary two-band conduction yields

$$\sigma_{xx} = n_1 e \mu_1 + n_2 e \mu_2 \tag{30}$$

Since $\rho_{xx} \cong \sigma_{xx}^{-1}$ in our samples, there is a slight increase in the number of carriers as temperature decreases as is shown in figure 6. This behavior is expected for a degenerate material.

Since the optical reflectivity suggests a band gap of ~0.08 eV, a band model shown in figure 7 is proposed. A degenerate n-type impurity band overlaps the conduction band.

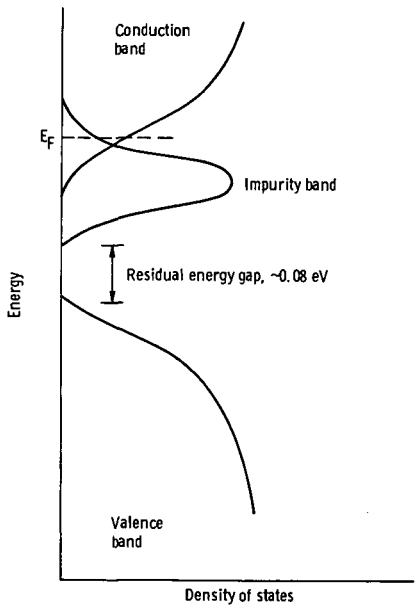

Figure 7. - Density of states model used to qualitatively explain data.

These bands are located at different positions in k space, and carrier compensation (as in a semimetal) can thus exist. From our analysis, the mobilities of the two bands are nearly the same. A band gap exists between the impurity band and the conduction band. Changes in optical reflectivity are then caused by optical excitation of carriers to the conduction band. Transmission experiments were not possible due to strong absorption.

The number of holes and the number of electrons could not accurately be found from the two-band model since high enough magnetic fields ($\gtrsim$18 tesla) were not available to make equation (16) applicable. An estimate of $n_1 + n_2$ was made, however, using equation (30) from the two-band model, and these values are listed in table I as a function of temperature. Then, knowing $a \cong 0.9997$, $n_1 \cong n_2 \cong 10^{25}$ meter^{-3}. These numbers are characteristic of semimetallic densities and are consistent with the model of a heavily doped semiconductor proposed. Since chemical analysis revealed very low concentrations of anything but bismuth and selenium, the impurity states are created by lack of stoichiometry.

CONCLUSIONS

It has been found that Bi_2Se_3 single crystals grown by the Bridgman technique are excellent Hall effect magnetometers for the temperature range 1.1 to 300 K and magnetic fields to at least 10 tesla. The slope of the ρ_{yx} against B curve varies by less than 1.0 percent in the temperature range 4 to 35 K. In the same temperature range, a copper magnetometer calibration changes by 100 percent. Quenching tests demonstrate magnetometer reliability for cryogenics applications.

Our samples of Bi_2Se_3 are highly degenerate with an impurity band partially filling the band gap of the intrinsic material. This leaves a band gap of approximately 0.08 eV. Conduction is found to be by at least two bands, with mobilities of about 0.056 square meter per volt per second, and near compensation of carriers.

To be useful as optical devices (lasers or radiation detectors, for example), crystals with greater stoichiometry need to be grown. This will reduce the free carrier optical absorption and increase the mobility. For possible laser use, the position of maxima and minima in the energy bands in k space must also be found. It is interesting that Bi_2Se_3 would not have been useful as a Hall effect magnetometer if the low mobility and lack of stoichiometry had not existed.

Lewis Research Center,
National Aeronautics and Space Administration,
Cleveland, Ohio, August 8, 1972,
503-10.

APPENDIX A

SYMBOLS

a	ratio of concentrations of two carriers, n_2/n_1
B	magnetic field
B_i	characteristic field of i^{th} carrier
b	ratio of mobilities of two carriers, $\mu_1/\mu_2 = B_2/B_1$
c	velocity of light
e	electronic charge
e_i	charge of i^{th} carrier
n	number of carriers per unit volume
n_i	number of carriers per unit volume for i^{th} carrier
$n_1 + n_2$	net carrier density
$R_H(B)$	Hall constant, ρ_{xy}/B
μ	mobility
μ_B	Hall mobility
μ_c	magnetoconductivity mobility
$\overline{\mu}_c$	average magnetoconductivity mobility
μ_i	mobility of i^{th} carrier
ρ_{xx}	resistivity
$\rho_{xx}(B)$	resistivity as function of B
ρ_{yx}	Hall resistivity
$\Delta\rho/\rho$	magnetoresistance
$\sigma_{xx}(B)$	conductivity at field B

APPENDIX B

DERIVATION OF EQUATIONS (19) AND (20)

Using equations (3) and (17) and definitions (11) and (12) gives

$$\rho_{xy} = \frac{\left(\frac{n_1 e}{B_1^2 M_1} - \frac{n_2 e}{B_2^2 M_1}\right) B}{\left(\frac{n_1 e}{B_1 M_1} + \frac{n_2 e}{B_2 M_2}\right)^2 + \left(\frac{n_1 eB}{B_1^2 M_1} - \frac{n_2 eB}{B_2^2 M_2}\right)^2} \tag{30}$$

$$\rho_{xy} = \frac{\frac{n_1 e}{B_1^2}\left(\frac{1}{M_1} - \frac{\frac{a}{b^2}}{M_2}\right) B}{\left(\frac{n_1 e}{B_1}\right)^2 \left(\frac{1}{M_1} + \frac{\frac{a}{b}}{M_2}\right)^2 + \left(\frac{n_1 eB}{B_1^2}\right)^2 \left(\frac{1}{M_1} - \frac{\frac{a}{b^2}}{M_2}\right)^2} \tag{31}$$

$$\rho_{xy} = \frac{\left(M_2 - \frac{a}{b^2} M_1\right) B}{\frac{n_1 e}{M_1 M_2}\left[\left(M_2 + \frac{a}{b} M_1\right)^2 + \left(\frac{B}{B_1}\right)^2 \left(M_2 - \frac{a}{b^2} M_1\right)^2\right]} \tag{32}$$

where M_i are defined by equation (21). Equation (32) then reduces to the desired expression

$$\rho_{xy} = \frac{\left[\frac{1}{b^2}(b^2 - a) + \left(\frac{B}{bB_1}\right)^2 (1 - a)\right] B}{n_1 e\left\{\left[\frac{M_2}{M_1} + \frac{2a}{b} + \left(\frac{a}{b}\right)^2 \frac{M_1}{M_2}\right] + \left(\frac{B}{B_1}\right)^2 \left[\frac{M_2}{M_1} - \frac{2a}{b^2} + \left(\frac{a}{b^2}\right)^2 \frac{M_1}{M_2}\right]\right\}} \tag{19}$$

It is easy (but lengthy) to show that if $B \ll B_i$ or if $a \simeq b \simeq 1$, then there will be no field dependence of the denominator.

Using equations (4) and (18) results in

$$\rho_{xy} = \frac{\dfrac{n_1 e}{B_1 M_1} + \dfrac{n_2 e}{B_2 M_2}}{\left(\dfrac{n_1 e}{B_1 M_1} + \dfrac{n_2 e}{B_2 M_2}\right)^2 + \left(\dfrac{n_1 eB}{M_1 B_1^2} - \dfrac{n_2 eB}{B_2^2 M_2}\right)^2} \tag{33}$$

$$\rho_{xx} = \frac{\dfrac{n_1 e}{M_1 M_2}\left(M_2 + \dfrac{a}{b} M_1\right)}{\dfrac{n_1 e}{B_1}\left(\dfrac{1}{M_1 M_2}\right)^2 \left(M_2 + \dfrac{a}{b} M_1\right)^2 + \dfrac{n_1 eB^2}{B_1^2}\left(\dfrac{1}{M_1 M_2}\right)^2 \left(M_2 - \dfrac{a}{b^2} M_1\right)^2} \tag{34}$$

$$\rho_{xx} = \frac{M_2 + \dfrac{a}{b} M_1}{\dfrac{n_1 e}{B_1 M_1 M_2}\left[\left(M_2 + \dfrac{a}{b} M_1\right)^2 + \left(\dfrac{B}{B_1}\right)^2 \left(M_2 - \dfrac{a}{b^2} M_1\right)^2\right]} \tag{35}$$

$$\rho_{xx} = \frac{\dfrac{B_1}{b}(a + b) + \left(\dfrac{B}{bB_1}\right)^2 (ab + 1)B_1}{n_1 e\left\{\dfrac{M_2}{M_1} + \dfrac{2a}{b} + \left(\dfrac{a}{b}\right)^2 \dfrac{M_1}{M_2} + \left(\dfrac{B}{B_1}\right)^2 \left[\dfrac{M_2}{M_1} - \dfrac{2a}{b^2} + \left(\dfrac{a}{b^2}\right)^2 \dfrac{M_1}{M_2}\right]\right\}} \tag{20}$$

REFERENCES

1. Coles, W. D.; Laurence, J. C.; and Brown, G. V.: Cryogenic and Superconducting Magnet Research at the NASA Lewis Research Center. Paper 21c presented at the AIChE 62nd Annual Meeting, Washington, D.C., Nov. 16-20, 1969.

2. Higgins, R. J.; and Chang, Yung K.: Simple NMR Probe for Use in Superconducting Solenoids. Rev. Sci. Instr., vol. 39, no. 4, Apr. 1968, pp. 522-523.

3. O'Sullivan, W. J.; and Schirber, J. E.: Acurate de Haas - van Alphen Periods for Calibration of Magnetic Fields at Low Temperatures. Cryogenics, vol. 7, no. 2, Apr. 1967, pp. 118-119.

4. Hudson, Wayne R.: Copper Magnetoresistance Devices as Magnetometers. NASA TN D-3536, 1966.

5. Veselago, V. G.; Glushkov, M. V.; Ivanov, V. M.; and Shul'man, S. G.: Film-Type Hall Transducers for Measuring Strong Magnetic Fields. Instr. Exper. Tech., no. 6, Nov.-Dec. 1969, pp. 1580-1581.

6. Sanford, Thomas B.: Hall Effect Devices as Magnetometers in Cryogenic Applications. NASA TN D-2272, 1964.

7. Champness, C. H.; Muir, W. B.; and Chiang, P. T.: Thermoelectric Properties of n-Type Bi_2Te_3-Bi_2Se_3 Alloys. Can. J. Physics, vol. 45, no. 11, Nov. 1967, pp. 3611-3626.

8. Harman, T. C.: The Physics of Semimetals and Narrow Band-Gap Semiconductors. D. L. Carter and R. T. Bate, eds., Pergamon Press, 1971.

9. Hashimoto, Kimio: Galvanomagnetic Effects in Bismuth Selenide Bi_2Se_3. J. Phys. Soc. Japan, vol. 16, no. 10, Oct. 1961, pp. 1970-1979.

10. Caywood, L. P., Jr., and Miller, G. R.: Anisotropy of the Constant-Energy Surfaces in n-type Bi_2Te_3 and Bi_2Se_3 from Galvanomagnetic Coefficients. Phys. Rev., B, vol. 2, no. 8, Oct. 15, 1970, pp. 3209-3220.

11. Greenaway, D. L.; and Harbeke, G.: Band Structure of Bismuth Telluride, Bismuth Selenide and Their Respective Alloys. J. Phys. Chem. Solids, vol. 26, 1965, 1585-1604.

12. Gilman, John J., ed.: The Art and Science of Growing Crystals. John Wiley & Sons, Inc., 1963.

13. Arends, J.; and Wright, R. C.: Ga-As Diodes as Temperature Sensors in Magnetic Fields. Cryogenics, vol. 9, no. 4, Aug. 1969, pp. 281-282.

14. Soule, D. E.: Magnetic Field Dependence of the Hall Effect and Magnetoresistance in Graphite Single Crystals. Phys. Rev., vol. 112, no. 3, Nov. 1, 1958, pp. 698-707.

NASA-Langley, 1972 —— 26 E-6805

NATIONAL AERONAUTICS AND SPACE ADMINISTRATION
WASHINGTON, D.C. 20546

OFFICIAL BUSINESS
PENALTY FOR PRIVATE USE $300

SPECIAL FOURTH-CLASS RATE BOOK

POSTAGE AND FEES PAID
NATIONAL AERONAUTICS AND SPACE ADMINISTRATION
451

U.S.MAIL

POSTMASTER: If Undeliverable (Section 158 Postal Manual) Do Not Return

"The aeronautical and space activities of the United States shall be conducted so as to contribute . . . to the expansion of human knowledge of phenomena in the atmosphere and space. The Administration shall provide for the widest practicable and appropriate dissemination of information concerning its activities and the results thereof."

—NATIONAL AERONAUTICS AND SPACE ACT OF 1958

NASA SCIENTIFIC AND TECHNICAL PUBLICATIONS

TECHNICAL REPORTS: Scientific and technical information considered important, complete, and a lasting contribution to existing knowledge.

TECHNICAL NOTES: Information less broad in scope but nevertheless of importance as a contribution to existing knowledge.

TECHNICAL MEMORANDUMS: Information receiving limited distribution because of preliminary data, security classification, or other reasons. Also includes conference proceedings with either limited or unlimited distribution.

CONTRACTOR REPORTS: Scientific and technical information generated under a NASA contract or grant and considered an important contribution to existing knowledge.

TECHNICAL TRANSLATIONS: Information published in a foreign language considered to merit NASA distribution in English.

SPECIAL PUBLICATIONS: Information derived from or of value to NASA activities. Publications include final reports of major projects, monographs, data compilations, handbooks, sourcebooks, and special bibliographies.

TECHNOLOGY UTILIZATION PUBLICATIONS: Information on technology used by NASA that may be of particular interest in commercial and other non-aerospace applications. Publications include Tech Briefs, Technology Utilization Reports and Technology Surveys.

Details on the availability of these publications may be obtained from:

SCIENTIFIC AND TECHNICAL INFORMATION OFFICE

NATIONAL AERONAUTICS AND SPACE ADMINISTRATION

Washington, D.C. 20546